Estimation of urban flood volume using Low-Impact Development methods and machine learning approach.

Yashar Dadrasajirlou
Semnan University
Hojat Karami (hkarami@semnan.ac.ir)
semnan
Alireza Rezaei
Semnan University

Research Article

Keywords: SWMM, LID, Urban Flood reduction estimation, Machine Learning

Posted Date: June 23rd, 2022

DOI: https://doi.org/10.21203/rs.3.rs-1638955/v1

Estimation of urban flood volume using Low-Impact Development methods and machine learning approach.

Yashar Dadrasajirlou[1], Hojat Karami[2*], Alireza Rezaei[3]

[1]Civil engineering Department, Semnan University, Semnan, Iran (Email: Dadras_yashar@semnan.ac.ir)

[2]Civil engineering Department, Semnan University, Semnan, Iran (Email: Hkarami@semnan.ac.ir)

[3]Civil engineering Department, Semnan University, Semnan, Iran (Email: a.rezaei@semnan.ac.ir)

*Corresponding author. E-mail address: Hkarami@semnan.ac.ir

Abstract:

In recent years, the growth of urbanization has increased the impermeable levels and has caused an increase in the volume of floods and peak flood discharges. Many types of research have been done in the field of implementing environmentally friendly methods to make the urban environment more natural and at the same time be effective in controlling urban floods. The use of Low Impact Development (LID) methods is one such study. But choosing the best designs from among these strategies has always been a vital problem for urban water system designers. One of the goals researchers in the field of urban hydrology is to find methods to determine the required volume reduction. In the present study, the hydraulic behavior of the surface water collection system in the Golestan town of Semnan has been simulated using Storm Water Management Model (SWMM). In the following, the performance of

implementing different proposed designs of three types of LID_ namely rain barrel (RB), infiltration trench (IT), and permeable pavement (PP) _ was investigated. These plans include seven general scenarios, each with ten different LID combinations. These plans include seven general scenarios, each with ten different LID combinations. The results of hydraulic studies indicate the effectiveness of the PP-RB scenario with an average reduction of 90% of peak discharge and an average reduction of 80% of total flood volume. Also, the weakest performance is related to the IT scenario with an average reduction of 60% of peak discharge and 47% of total flow volume. In this regard, the considering the importance of estimation of flood reduction, present paper introduces a novel approach for urban flood mitigation estimation. In this method, intelligent algorithms are used to perform flood calculation operations taking into account the percentage of LIDs (Low-Impact Developments) proposed. In this research, SVM (support vector machines), LSSVM (Least square support vector machines) and LSSVM-GOA (Least square support vector machines-grasshopper optimization algorithm) algorithms have been used. The allocated percentage area of different combinations of the used LIDs, and the reduced peak flow coefficient in each combination were considered as input data; and the reduced flood volume corresponding to each LID combination was used as the output data. This research has been conducted in Golestan town of Semnan city in Iran. The results obtained in this study indicate the success of these algorithms in predicting reduced flood volume. In the test period, the value of R^2 index for LSSVM-GOA model (0.9896) compared to LSSVM (0.9266) and SVM (0.8990) intelligent models, indicates the high accuracy of this model in this period. Also, the values of R^2 index for the other two algorithms indicate the adequacy of these algorithms in predicting the amount of reduced flood. Also in the training course, LSSVM - GOA model showed that with values of 0.0101 and 0.0185 for MAE and RMSE indices, respectively, has a higher predictive power. The values of these indices are 0.0268 and 0.0361 for LSSVM model and 0.0318 and 0.0434 for SVM model,

respectively. According to the results, the use of intelligent algorithms can be introduced as an accurate tool in estimating and predicting reduced flood volume in urban basins.

Keywords: SWMM, LID, Urban Flood reduction estimation, Machine Learning

Introduction

Today, more than half of the world's population lives in urban areas (UN, 2012), and most of the world's population growth also occurs in cities (Flood, 1997). These changes have caused floods to have more severe effects on residential areas and urban infrastructure. These effects include drastic changes in runoff quality and quantity due to storm rains (Jacobson, 2011; Shen et al., 2014; Huang et al., 2018). Numerous studies have shown that urban development increases surface runoff (Dietz and Clausen, 2008; Schoonover et al., 2006; Wang et al., 2005; Palla and Gnecco, 2015). In recent years, many urban designers facing the challenge of urban flooding (Bisht et al., 2016). However, Floods causes significant damage, having proper management runoff can be used in semi-arid and arid regions (Ghazavi et al., 2012; Huang et al., 2018).

Mathematical models can achieve the best possible design for urban runoff management (Faye et al., 2016). Rainfall-runoff models either act on the occurrence of an event or continuously perform simulation. Event-based models usually perform rainfall-runoff calculations based on a unique short-term event. These models usually simulate only part of the hydrological processes of the catchment. Most event-based models use fixed time steps for hydraulic and hydrological analysis. Among all event-based models, the Storm Water Management Model (SWMM) is one of the most widely used mathematical models in the field of rainfall-runoff modeling in urban areas (Shahed Behrouz et al., 2020). The SWMM model was first introduced by the U.S. Environmental Protection Agency in 1971. Based on the environmental plan of the study area, SWMM simulates the rainfall-runoff of the basin and prepares the results of

quantitative and qualitative analyzes related to runoff (Faye et al., 2016). The SWMM model was used to simulate and calibrate storms observed in a large basin in Tallinn, and the results showed that the SWMM model is sensitive to the percentage of impermeable areas, flow volume, and peak discharge (Maharjan et al., 2017). Based on previous research studies, the SWMM model can estimate flood volume and peak discharge in urban sub-basins. In recent years, new methods for flood control in urban watersheds have been studied by researchers. One of the advantages of these new methods is being friendly to the environment. Green Infrastructure (gi), Best Management Practices (BMPs), and Low-Impact Development methods (LID) are among these methods (Eckart et al., 2012; Jia et al., 2015). However, to optimize LID and the costs allocated to these methods, appropriate optimization measurements should be used, especially when there are multiple criteria for decision making (Babaei et al., 2018). Recently, the use of LID has been introduced as a completely reliable method in controlling urban runoff, surface water pollution in the urban basin, and urban ecosystem. (Teymouri et al, 2020) (Kayhanian et al., 2012; Ahiablame et al., 2012; Randhir and Raposa, 2014). LIDs are a green approach to urban flood management. LIDs seek to assist in the hydrology of the urban basin, and this assistance is implemented on a small scale in the urban basin. (HUD, 2003). However, the use of these methods requires further experimental studies to determine the exact characteristics of these methods to make them more effective in controlling floods and peak discharges. The first goal of using LID in urban environments is to control urban floods by reducing possible runoff with a specified return period (Park et al., 2013). Mathematical models can be used to determine the type of LID and its location, especially when there is a limited budget for urban flood management (Prez-Pedinin et al., 2005), and also these models can be more effective in the wider use of LIDs (Elliott and Trowsdale, 2007).

The main idea is to use the LID method to control runoff and reduce pollution on site. There are different types of LIDs such as bio-retention cells, rain gardens, green roofs, rain barrels, Infiltration trenches, permeable pavements, roof separation, and green swale (Hoang and Fenner, 2016). One of the complexities of using LID methods is the optimization of the space allocated to them and their implementation costs (Martin-Mikle et al., 2015; Geng and Sharpley, 2019). The purpose of implementing the LID-BMPs is to reduce the volume of floods and to create the natural hydrology of the water basin as much as possible. However, the optimization of LIDs will be commensurate with their performance by considering criteria such as effectiveness in reducing the quantity of flood volume, improving the quality of urban runoff, physical constraints of the area, implementation costs, and even social factors.

Increasing urbanization rates in the world have caused impermeable surfaces to replace permeable soils (Zhang et al., 2015). The spread of impermeable areas parallel with climate change has caused considerable increase in flood volume in urban residuals (Olang and Furst, 2011; Zhang, W. et al., 2018). In other hand, the occurrence of heavy rainfall challenge the urban wastewater drainage system and thus have major impacts on communities, habitats and the economy (li et al., 2020). The complexity of the urban environment necessitates integrated research and policies to control urban flooding (Lawson et al., 2014; Pappalardo et al., 2017). In recent years, various methods for modeling and predicting flood rates have been proposed by researchers (Henonin et al., 2015; Mark et al., 2004; Miguez et al., 2017; Rene et al., 2014). Nature-based solutions, known as green infrastructure, have been widely recommended for reducing runoff from urban flooding, improving water quality, and having a sustainable ecosystem (Fu et al., 2019). It has been reported that among the various methods of urban flood management, green infrastructure has a better performance in reducing runoff and peak discharge (Wolch et al., 2014). The effectiveness of green infrastructure in reducing urban flooding is affected by a combination of several factors such as: the study area, the distribution

of green infrastructure in the region, and the hydraulic characteristics of green infrastructure (Fiori and Volpi, 2020). Floods are one of the most well-known devastating natural disasters in the world (Freer et al., 2013; Razavi et al., 2020). However, floods can be useful in supporting ecosystems, especially in areas with arid climates (Teng et al., 2017; Bond et al., 2014). Therefore, considering all the positive and negative aspects of floods, it can be concluded that understanding, simulating, predicting and evaluating floods is of great importance (Teng et al., 2017).

In recent years, intelligent models have been used extensively in modeling and predicting hydraulic and hydrological phenomena. For example, use of support vector machine to predict flood sensitivity (Choubin et al., 2018, Karami et al, 2022), using LSSVM, a new method for correcting runoff prediction error (Liu et al., 2021), using variational mode decomposition and the least squares support vector machine optimized by the sparrow search algorithm (VMD-SSA-LSSVM) to predict the water quality of the Yangtze River (Song et al., 2021), using whale optimization algorithm and combining it with LSSVM to subscale rainfall prediction under climate change conditions (Valikhan Anaraki et al., 2021), application of SVM and LSSVM to modeling of evaporation from open water surfaces (Farasat et al., 2021), using Coupling Singular Spectrum Analysis with Least Square Support Vector Machine to improve the accuracy of SPI drought forecast index (Pham et al., 2021), precipitation modeling by optimizing performance and LSSVM (Azad et al., 2021), using complementary ensemble empirical decomposition models and combining it with LSSVM to predict runoff in the medium and long term (Ji et al., 2020), using MSPI and data DRIVEN methods to detect multivariate droughts in the short and long term (Aghelpour et al., 2021), comparison of SVM and ANFIS performance for daily dam water level forecasting (Hipni et al., 2013), using Extreme Learning Machine in SVM Composition to Predict Hydrological Flow Series (Atiquzzaman and Kandasamy 2018), using SVM to predict long-term flow (Lin et al., 2006),

evaluation of SVM and ANN performance in runoff modeling (Behzad et al., 2009), using SVM to estimate soil moisture (Gill et al., 2007), using SVM to estimate and predict evaporation rate (Moghaddaminia et al., 2009), investigation of statistical subscales on daily rainfall using SVM (Chen et al., 2010), using SVM to simulate and analyze runoff and sediment (Misra et al., 2009), using SVM to predict scour on control grade structures (Goel and Pal., 2009), a comparative study between ANN and SVM performance for groundwater level prediction in coastal aquifers (Yoon et al., 2011), monthly forecast of evaporation using ANN and SVM (Tezel and Buyukyildiz, 2015), using ANFIS and SVM to predict the relationship between runoff-precipitation (Tasar et al., 2019), combining improved GOA and SVM algorithms to predict water levels in streams in coastal areas (Tao et al., 2021), combination of SVR and GOA for spatial prediction of flood occurrence in Qazvin plain (Panahi et al., 2021).

A review of previous studies shows that research has been done in the field of flood prediction using intelligent algorithms, but in the field of flood reduction prediction using hybrid algorithms and using the percentage of available LIDs as research input has not yet been conducted enough. This study introduce a new solution to find the best percentage of LIDs used in urban areas to further reduce floods in the area using SVM, LSSVM and LSSVM-GOA algorithms. In this research, in the materials and methods section, the study area is introduced, the modeling of the area in software, SWMM field, and input and output data are introduced. Then the following algorithms are introduced. In the results and discussion section, the performance of these three algorithms is examined using statistical parameters, and finally, in the conclusion section, the total achievements of this research and future work suggestions are introduced. The process used in this study presented in figure 1.

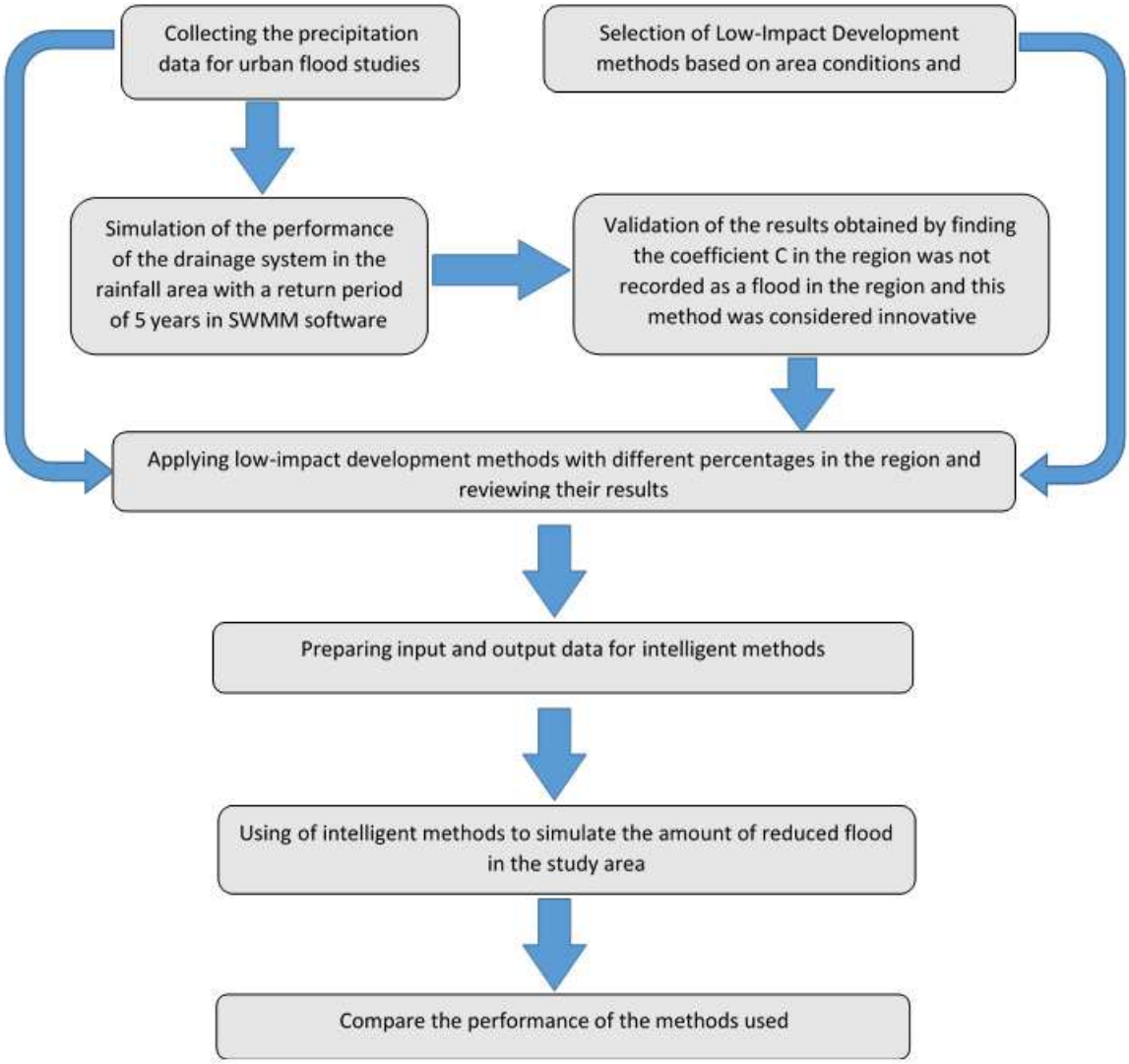

Figure 1-. The flowchart of the study

Materials and methods

Study area

Golestan town is in the northern part of Semnan city located in Semnan province. Considering the residential settlements in this area of the city, it is considered as one of the centralized areas in the city of Semnan. The study area locates at northwest of Semnan city with an area of about 2.86 Km (285 hectares). The maximum and minimum heights of the area are 1243.73 and 1175 meters, respectively. The city of Semnan is located in the north of the desert plain and south of

the Alborz mountain range. The city is located at longitude 53 degrees, 23 minutes to 53 degrees and 26 minutes east and latitude 35 degrees and 33 minutes to 35 degrees and 35 minutes north. Its average altitude is 1132 meters above sea level. Figure 2 shows the location of Semnan province and Semnan city and Figure 3 shows Golestan region in the north of Semnan city.

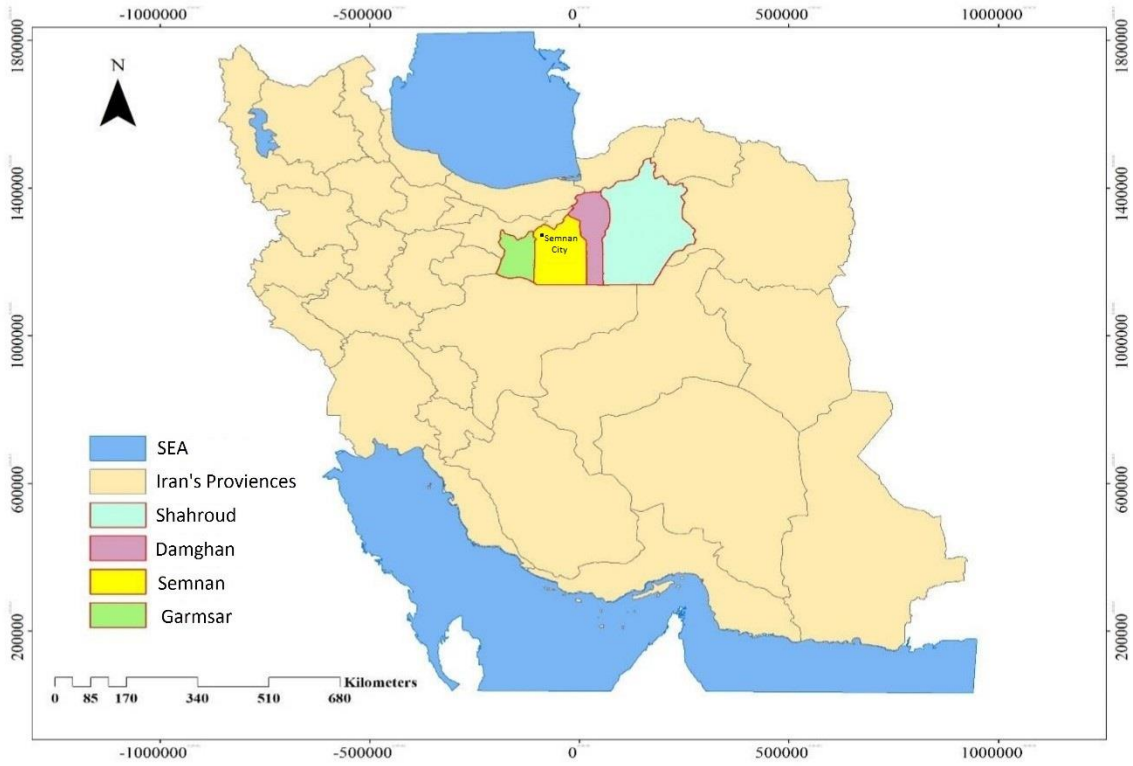

Figure 2- Geographical location of Semnan province and Semnan city

Figure 3- Golestan town area in the north of Semnan city

Hydrologic modeling with SWMM

According to the available information of the area, the modeling of the Golestan area was done in SWMM software, and the amount of peak runoff and runoff volume was recorded in the outlet of the basin. Due to the fact that there was no historical flood records in the area, the model was calibrated and validated only with the peak flow obtained from the software and compared with the peak flow calculated from the logical relation (Formula 2) in each of the sub-catchment. Considering that each sub-catchment was composed of different land uses, initially the area of different parts of each sub-catchment was calculated using AutoCAD software. Then by using relative weight averaging (Equation 1) to the area of each sub-catchment, the runoff coefficient of each sub-catchment was calculated.

$$\bar{C} = \frac{\sum_{i=1}^{n} C_i A_i}{\sum_{i=1}^{n} A_i} \tag{1}$$

In the above relation Ci is the value of the runoff coefficient related to the area Ai of each sub-catchment. After calculating the value of $\bar{C}$ for each sub-catchment using the logical formula (Equation 9), the peak flow rate in each sub-basin was calculated:

$$Q = 0.278 * C * i * A \tag{2}$$

Which Q stands for maximum peak discharge (m^3/s), C is the runoff coefficient, i is rainfall intensity (mm/hr), and A is the area of catchment (km^2).

The coefficient of determination (R^2) (equation 3) (Band et al., 2021) and root mean square error (RMSE) (equation 4) (Hu et al., 2021) were used to evaluate the validation of the the process.

$$R^2 = \left[\sum_{i=1}^{n} (x_i - \bar{x})(y_i - \bar{y}) \Big/ \sqrt[2]{\sum_{i=1}^{n} (x_i - \bar{x})^2 \sum_{i=1}^{n} (y_i - \bar{y})^2} \right]^2 \tag{3}$$

$$RMSE = \sqrt{\sum_{i=1}^{n} (x_i - y_i)^2 / N} \tag{4}$$

Which in the above relations x_i and $\bar{x}$ express the observational values and their averages; y_i and $\bar{y}$ also represent the predicted values and their mean.

Figure 4 shows the value of the R^2 between the peak flow values calculated with the logical formula and the peak flow simulated with the SWMM for the 5-year return period. According to R2 = 0.8657 and RMSE = 0.01653(m^3/s), it can be concluded that the SWMM model has shown a good ability to simulate the runoff collection system in the study area.

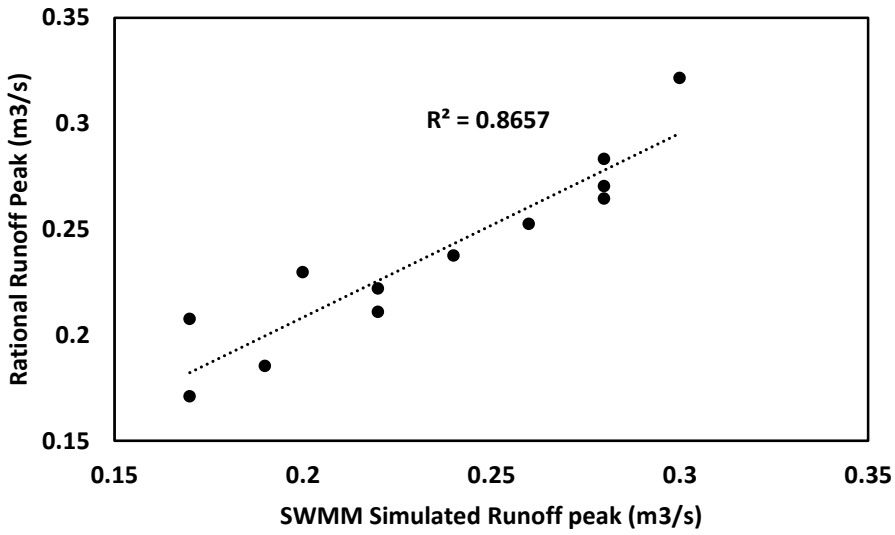

Figure 4 - Peak discharge obtained from the logical equation and peak runoff calculated by SWMM

The seven scenarios include three individual scenarios, three pair scenarios, and one general scenario. Each one contains ten different plans. Table 4 shows how to name the plans. The maximum flood volume and maximum runoff for the outfall point were considered as model outputs.

Modeling the study area in the current conditions

Figure 5 is a schematic view of the runoff collection system in Golestan town. The initial modeling results indicate the phenomenon of flooding in one of the nodes. Tables 1 and 2 show the hydraulic output results for the output node and the flood node, respectively, taking into account the total volume in the node as well as the maximum flow.

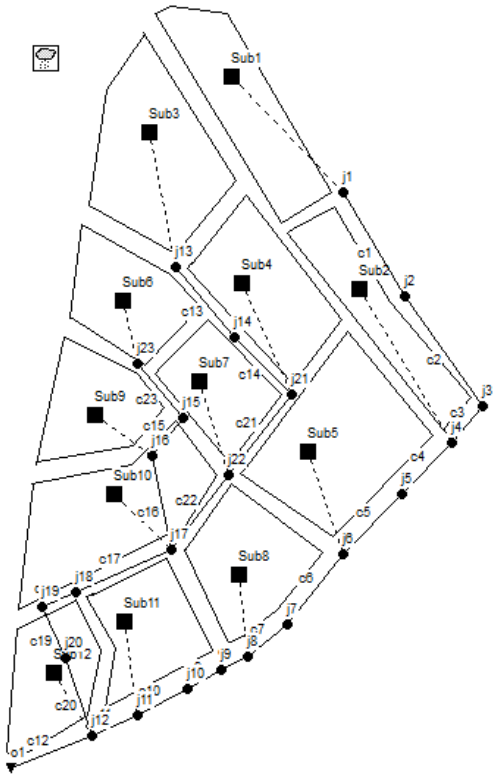

Figure 5- Schematic of runoff collection system

Table 1: Hydraulic output of the output point (O1) in the current condition

Runoff peak (m^3/s)	Total volume of flow (10^6 lit)
0.559	3.446

Table 2: Hydraulic output node 18 (J18) in the current condition

Runoff peak (m^3/s)	Total volume of flow (10^6 lit)
0.569	1.281

Low-Impact development Methods

Storm water is usually water that does not penetrate the ground, but flows on the ground and impermeable surfaces and flows into streams, rivers, lakes, etc. Low-impact development methods used to reduce flood volume and peak discharge in this area include rain barrels (RB), permeable pavement (PP), and infiltration trench (IT). These methods have been selected

according to the arid and semi-arid climate of the region, and the available materials which their specifications are presented in table 3.

Table 3 - Lid specifications

LID type	LID features	amount
Rain Barrel	Barrel height (mm)	1000
	Flow coefficient	0.8
	Flow exponent	0.5
	Offset (mm)	6
	Drain daily (hrs)	6
Permeable pavement	Surface roughness	0.12
	Thickness (mm)	120
	Void ratio	0.6
	Flow coefficient	0.8
	Flow exponent	0.5
	Offset (mm)	15
	Soil conductivity (mm/hr)	120.4
	Soil thickness (mm)	150
	Storage thickness (mm)	250
Infiltration Trench	Surface slope (%)	1
	Storage thickness (mm)	1000
	Void Ratio	0.75
	Flow coefficient	0.8
	Offset (mm)	6

The seven scenarios include three individual scenarios, three pair scenarios, and one general scenario. Each one contains ten different plans. Table 4 shows how to name the plans. The

maximum flood volume and maximum runoff for the outfall point were considered as model outputs.

Table 4 -LID Scenarios

scenario	type	Number of plans	symbol	Example	Explanation of Example
1	individual	10	RB-Usage percentage	RB-30	The LID used is a rain barrel, and the percentage used is 30%
2	individual	10	PP-Usage percentage	PP-20	The LID used is a permeable pavement, and the percentage used is 20%
3	individual	10	IT-Usage percentage	IT-70	The LID used is an infiltration trench, and the percentage used is 70%
4	Paired composition	10	IT-PP-Usage percentage	IT-PP-35	The LIDs used are permeable pavement and infiltration trench, and the percentage used of each of them is 35%.
5	Paired composition	10	IT-RB-Usage percentage	IT-RB-15	The LIDs used are infiltration trench and rain barrel, and the percentage used of each of them is 15%.
6	Paired composition	10	PP-RB-Usage percentage	PP-RB-45	The LIDs used are permeable pavement and rain barrel, and the percentage used of each of them is 35%.
7	Triple composition	10	IT-PP-RB-Usage percentage	IT-PP-RB-20	The LIDs used are of all three types, and the percentage used of each of them is 20%

The results of the hydrologic modeling in SWMM

This section briefly discusses the results of hydrological analysis of various LID scenarios. As can be seen from Table 4, 7 different scenarios of ineffective development methods were considered. In between, each of the scenarios has 10 different models that differ in the percentage of LID used. Comparing the results of the RB scenario, it was found that the lowest rate of peak flow reduction and flood volume is related to the RB-10 project with approximate values of 74.5% and 79% and the highest values of these two parameters are related to the RB-100 design with approximate values of 79.5% and 83%. PP scenarios have succeeded in gradually reducing the volume of floods so that a reduction of 1.4 million liters can be observed, while the maximum flow in PP-80, PP-90, AND PP-100 ARE about 0.15 m^3/s. The performance of IT scenarios and PP scenarios in reducing peak discharge are similar to each other, with the difference that IT scenario have smaller values of peak discharge compared to PP scenario. According to the results of IT scenario (IT-10 and IT-100), it can was seen that increasing the percentage of IT coverage in the sub-catchments plays important role in reduction of the peak discharge and flood volume. The SWMM results showed that increasing the percentage of combined coverage of IT and PP has a significant ability to control the amount of runoff. So that the values of total flood volume and maximum flow for IT-PP-5 and IT-PP-50 projects are equal to 2.674 million liters, 0.387 (m^3/s), 1.011 million liters, and 0.062 (m^3/s), respectively. Successful plans of this scenario (IT-PP-45 and IT-PP-50) have reduced about 90% of peak discharge and 70% of flood volume. The results obtained from this scenario show that the combination of IT and PP can cover each other's problems and represent better hydraulic performance than individual scenarios. Simultaneous use of RB and PP has had acceptable results in flood control in the study area. According to the obtained results, increasing the percentage of these two LIDs has a significant effect on controlling urban runoff. The obtained results from SWWM considering PP and RB as a combination of LIDs shows

that the percentage reduction for peak discharge and flood volume is between 80 and 98% for peak discharge and 70 to 90% for flood volume. While considering all three Lid methods together, the results show that this scenario is effective in reducing the flood's volume and peak discharge. The SWMM results showed that the PP-RB scenario has recorded the lowest peak flow rate at the output point. The RB scenario, the IT-RB scenario, and the IT-PP-RB scenario are in the next ranks in terms of peak discharge, respectively. While the highest peak discharge at the output node is related to the IT scenario. The PP-RB scenario has the best performance, and the IT scenario has the worst. Also, the IT-PP-RB and IT-RB scenarios as well as the IT-PP and RB scenarios have shown considerable performance in the total runoff volume. The PP-RB scenario has shown the best hydraulic performance by recording an average of 90% reduction in peak discharge and 80% reduction in flood volume, while the weakest results are obtained in the IT scenario with an average decrease of approximately 60% in peak discharge and 40% in flood volume. The results show the similar performance of the two scenarios IT-PP-RB and IT-RB in reducing the peak discharge by 80 percent. Also, the three scenarios of RB, PP, and IT-PP have shown similar results in reducing the peak flow rate (75%).

Data used for intelligent methods

The input data of the model includes the percentage of LIDs and K coefficient. The LIDs used were in three general modes. In other words, either the LID was used individually or a binary combination and a ternary combination was used. Finally, the area of LIDs as a percentage was used in this study. To use the K coefficient, it was necessary to consider the rate of peak flow reduction associated with each mode compared to the non-LID mode. The reduced flood volume in each case was also considered as output data for the model. The study area includes 12 sub-areas. The range of data used is shown in the table 5.

Table 5- Statistical details of input and output data used in this research

	input				output
	Percentage of rain barrel	**Percentage of porous pavement**	**Percentage of infiltration trench**	**$K_{Q\text{-}peak}$**	**Percentage of flood reduction**
Max	100	**100**	**100**	0.782363977	79.01915264
Min	0	**0**	**0**	0.786116323	79.48345908
Average	18.286	18.286	18.286	0.818198874	65.87588094

Support vector machine

Vapnik introduced support vector machine in 1995 (Vapnik, 1995).

The biggest positive feature of this algorithm is that it does not fall into the trap of local optimization using global optimization methods in its structure. The Support vector machine algorithm also maps the input vector to a higher dimensional space using a nonlinear function. By using linear regression, SVM calculates the amount of output. It is assumed that (x, y) are observational period data where x is the input vector and y is the observational output. Equation 5 formulates the linear regression as follow:

$$y' = f(x) = \omega^T \phi(x) + b \tag{5}$$

Where f (x) represents the linear relationship, and $\phi(x)$ represents the nonlinear mapping function. ω and b also represent the weight and bias. In order to reduce the difference between the model outputs and the actual outputs, it is necessary to minimize Equation 6:

$$\min : \psi = \tfrac{1}{2}\|\omega\|^2 + \gamma \sum_{i=1}^{n} (\xi_i + \xi_i^*)$$

$$subject\ to : \begin{cases} \omega\phi(x_i) + b - y \le \varepsilon + \xi_i \\ y - \omega\phi(x_i) + b \le \varepsilon + \xi_i^* \\ \xi_i, \xi_i^*, i = 1,2,3...,n \end{cases} \quad (6)$$

In the first term of this relationship, $\tfrac{1}{2}\|\omega\|^2$ is the norm of the weights. The second term, γ, is a real positive number showing penalty coefficient, ξ_i and ξ_i^* are also the penalty coefficients of the upper and lower error The accuracy of the model is indicated by the parameter ε. Therefore, model simplicity and experimental error are indicated by the first and second expressions, respectively. In this research, the radial kernel function has been used (Equation 7):

$$K(x, x_i) = \exp\left(\frac{-\|x - x_i\|^2}{2\sigma^2} \right) \quad (7)$$

σ indicates the width of the kernel function and K represents the nonlinear kernel function.

Least Square Support Vector Machines (LSSVM)

Suykens first introduced the support vector machine (Suykens 2001). The reason for the short computation time in LSSVM compared to SVM is the change in optimization method. In other word, the nonlinear relationship between inputs and outputs becomes a linear relationship by considering the mapping from lower dimension space to higher dimension space (Suykens 2001). This is one of the most practical methods of solving nonlinear problems (Anandhi et al., 2008). The linear relation expressed in LSSVM is formulated in Equation 8:

$$y' = W^T \Phi(x) + b \quad (8)$$

W: weight of the inputs

b: Bias

φ: mapping onlinear function

x: input

y: output

By minimizing Equation 5, the difference between modeled data and real data is reduced to its lowest value: (Anandhi et al., 2008)

$$\begin{aligned} &Min: \Psi(W,e) = \frac{1}{2}W * W^T + \frac{1}{2}C\sum_{i=1}^{N} e_i \\ &Subject\ to: e_i = y_i - y'_i \end{aligned} \tag{9}$$

In Equation (9) the coefficient C is used to apply the penalty coefficient and has a positive and fixed value. If the value of coefficient C is high, it causes the complexity of the equation, and if its value is low, it reduces the complexity of the equation. The first part of Equation (9) is used to show the norm of weights. In other words, the value of this part is directly related to the complexity of the problem, so if its value decreases, it means that the problem is less complex.

Grasshopper optimization algorithm

The GOA is a new intelligent optimization method that was introduced to by Saremi et al. to solve complex engineering problems (Saremi et al., 2017). This algorithm has advantages compared to other optimization algorithms such as the participation of all search agents in updating the position of each search agent, special attention to avoid falling into the trap of local optimization and convergence, balance global and local search capabilities, no need for information is the gradient of the search space (Saremi et al., 2017). In this algorithm, the position of the Grasshoppers in the group is defined as Equation 10:

$$X_i = S_i + G_i + A_i \tag{10}$$

In this regard, S_i is the effect of social interaction, G_i is the effect of gravity, and A_i is the effect of wind on the movement of the grasshopper. Equation 11 is used to simulate the social interaction of grasshopper:

$$S_i = \sum_{j=1} s(d_{ij}) d'_{ij} \tag{11}$$

In this relation, d_{ij} represents the Euclidean distance between the ith and the jth grasshoppers, s is the stress due to the community force, and d'_{ij} is the unit vector, which indicates the direction of the movement of the ith grasshopper towards the jth grasshopper. The function is defined as Equation 12:

$$S(r) = fe^{-r/l} - e^{-r} \tag{12}$$

In this relation, f is the absorption intensity and l is the absorption length scale. In this equation, two forces of absorption and repulsion are considered. When the distance of the grasshoppers from each other is between 0 and 2.079, the force of them is repulsive and when this distance is between 2.079 and 4, this force is gravitational. Also, if the distance is 2.079, no force is created (Saremi et al., 2017). Equation 13 shows the formula for updating the position of the grasshoppers:

$$X_i^d = c\left[\sum_{j=1}^{n} c((ub_d - lb_d)/2).s(|x_j^d - x_i^d|)\frac{x_j - x_i}{d_{ij}}\right] + T_d \tag{13}$$

In this relation, ub and lb represent the upper limit and the lower limit of the decision variables, respectively. T indicates the goal or best position achieved so far. Parameter c also represents a decreasing coefficient to limit the neutral zone, repulsion zone and gravity zone. The c parameter causes the group of grasshoppers to converge towards the target. This position, which is followed by a group of grasshoppers, will be updated if a new position is found. Equation 14 represents the formula for updating the parameter in each iteration:

$$c = c_{\max} - l\,(c_{\max} - c_{\min})/L \tag{14}$$

In this regard, L represents the maximum number of iterations, l the current number of iterations, c_{max} = 1 and c_{min} = 0.00001.

Least Square Support Vector Machines-Grasshopper optimization algorithm

In the present study, a hybrid of LSSVM-GOA has been used to predict Volume Reduction.

The process of this hybrid method is described below: (Figure 6)

1) The basic parameters of GOA such as population, frequency, number of repetitions are determined.

2) Preparing training data and test data

3) Production of the initial population

4) Training LSSVM and decision variables of GOA using training data

5) Test LSSVM and determine the target function of GOA

6) Check the termination conditions; if the termination conditions is satisfied, return the optimal values of the LSSVM parameters, otherwise change the position of each Grasshopper and repeat steps 4 and 5.

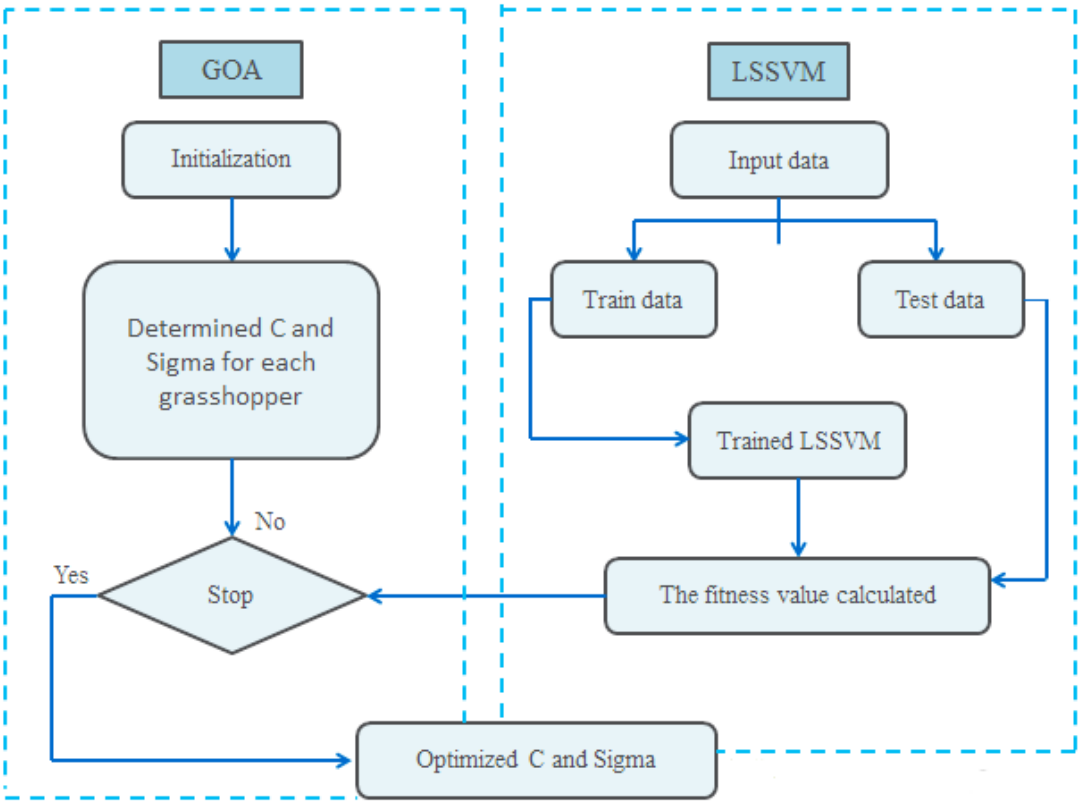

Figure 6- Flow chart of LSSVM-GOA algorithm

Statistical indicators

To determine the accuracy of Volume Reduction (VR) predicted by intelligent models evaluation indicators including coefficient of determination (R^2), mean square error (MAE), root mean square error (RMSE) respectively according to the relations (15), (16) and (17) are used. The coefficient of determination indicates the degree of correlation between the real data and the modeled data of the intelligent model, and the closer the value is to one, indicates that there is a good correlation. The MAE and RMSE indices show the rates of error, and the closer the value of these indices is to zero, the more precise the predicted values are.

$$R^2 = 1 - [\frac{\sum_{i=1}^{n}(E_i - G_i)^2}{\sum_{i=1}^{n}(E_i)^2 - \frac{\sum_{i=1}^{n}(G_i)^2}{N}}] \quad (15)$$

$$MAE = \frac{1}{N}\sum_{i=1}^{n}|E_i - G_i| \tag{16}$$

$$RMSE = \sqrt{\frac{\sum_{i=1}^{n}(E_i - G_i)^2}{N}} \tag{17}$$

In the above relations, E_i is the value real data, G_i is the estimated value, and N is the number of data.

Results and discussions

Figure 7 shows the results of Volume Reduction (VR) prediction in two train and test courses for SVM, LSSVM and LSSVM-GOA models. The results show that in the training course, the LSSVM-GOA model with an R^2 value of 0.9874 is superior to the SVM model with a value of 0.9483 and the LSSVM model with a value of 0.8977. Regarding MAE and RMSE indices in this period, LSSVM-GOA model with values of 0.0124 and 0.0209, respectively, has shown better performance compared to SVM model with values of 0.0234 and 0.0422, and LSSVM model with values of 0.0418 and 0.0594. In the test period, the higher value of R^2 for LSSVM - GOA model (0.9896) than LSSVM (0.9266) and SVM (0.8990), indicates the high accuracy of this model in this period.

Also, in this period, LSSVM - GOA model showed higher predictive power with values of 0.0101 and 0.0185 for MAE and RMSE indices respectively, compared to LSSVM model with values of 0.0268 and 0.0361 and SVM model with values of 0.0318 and 0.0434.

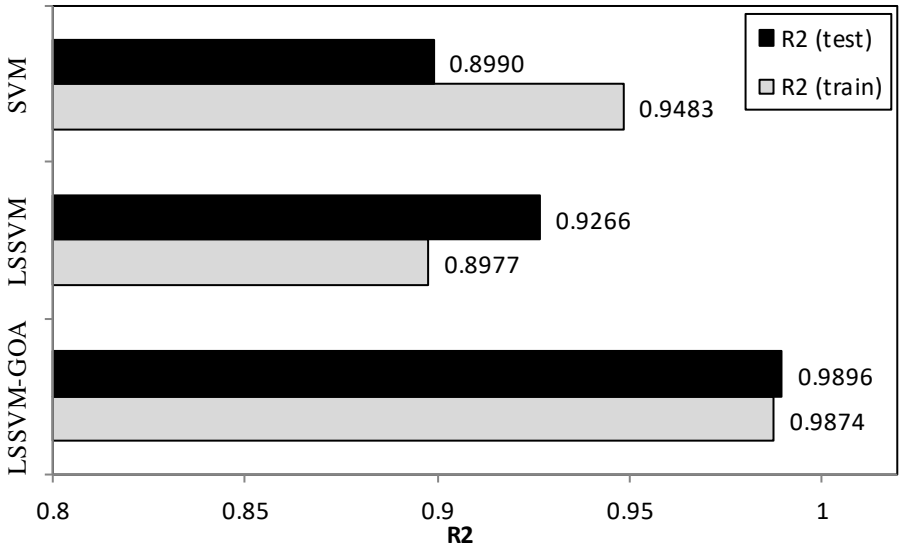
R2 (test)
R2 (train)
SVM
LSSVM
LSSVM-GOA
0.8990
0.9483
0.9266
0.8977
0.9896
0.9874
0.8
0.85
0.9
0.95
1
R2

(a)

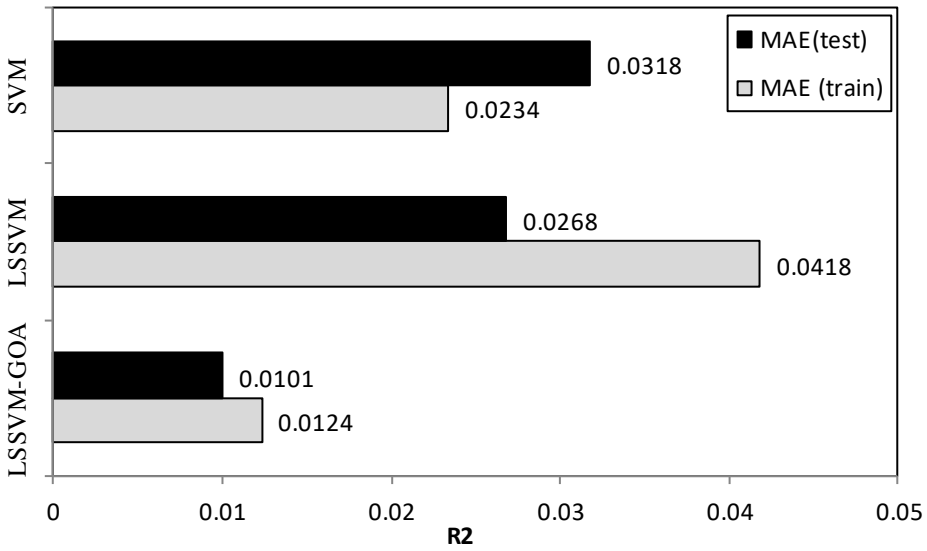
MAE(test)
MAE (train)
SVM
LSSVM
LSSVM-GOA
0.0318
0.0234
0.0268
0.0418
0.0101
0.0124
0
0.01
0.02
0.03
0.04
0.05
R2

(b)

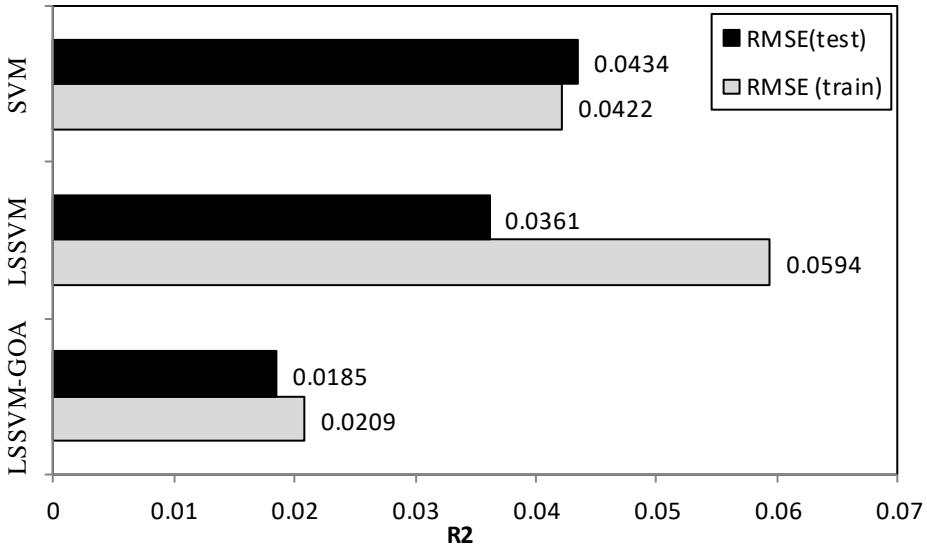

(c)

Figure 7 – Comparison of models in estimating the Flood Volume Reduction during training and testing phases: a) R^2 , b) MAE, c) RMSE

Figure 8 showed the estimated DR for the LSSSVM-GOA, LSSVM, and SVM models. The DR parameter is the result of dividing the predicted values by the intelligent model (G_i) into experimental values (E_i) ($DR = \frac{G_i}{E_i}$). Figure 3 shows the DR value distribution for these models in the training course. For example, the DR_{max}, DR_{min}, and DR_{ave} values for the LSSSVM-GOA model are 1.2207, 0.8529, and 1.0048, respectively. However, the DR_{max} values for the LSSVM and SVM models are estimated at 1.4328 and 1.3518, respectively. Also, for LSSVM and SVM models, DR_{min} is 0.7705 and 0.7736, respectively. It should be noted that DR_{ave} for LSSVM and SVM models is 1.0157 and 1.0085, respectively.

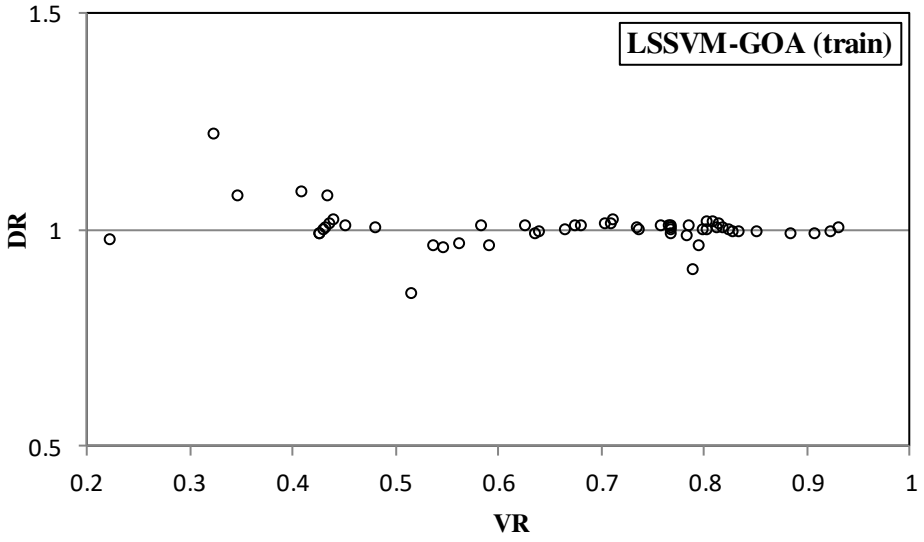
LSSVM-GOA (train)
DR
VR
1.5
1
0.5
0.2
0.3
0.4
0.5
0.6
0.7
0.8
0.9
1

a

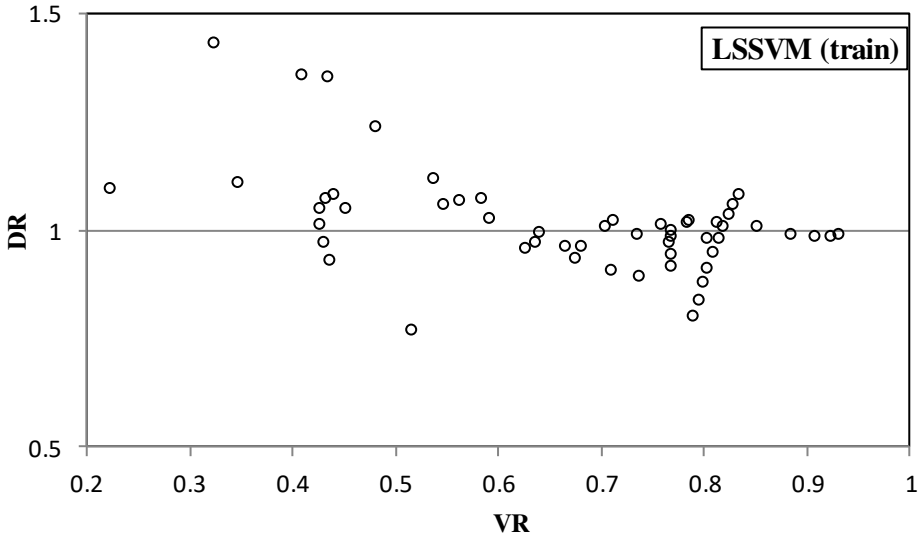
LSSVM (train)
DR
VR
1.5
1
0.5
0.2
0.3
0.4
0.5
0.6
0.7
0.8
0.9
1

b

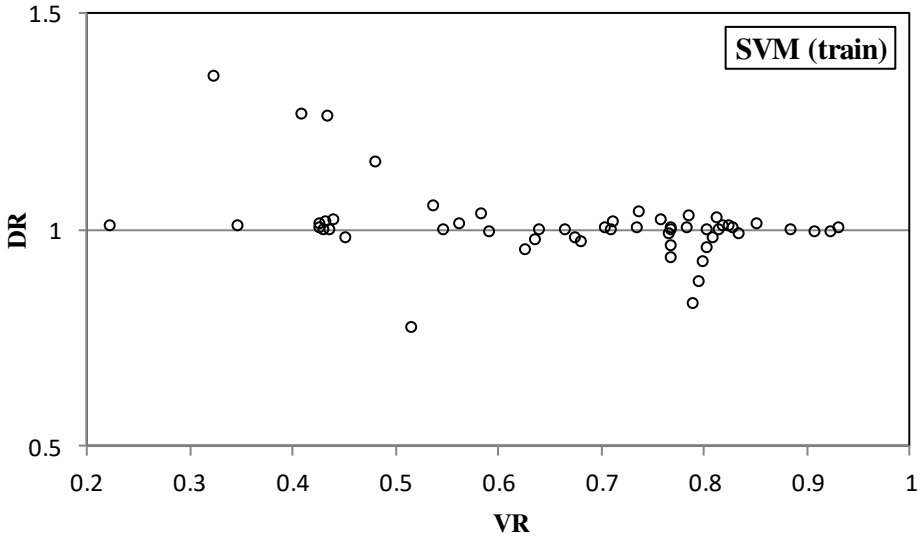

c

Figure 8- DR graphs in the training phase for models: a) LSSVM-GOA, b) LSSVM, c) SVM

Figure 9 shows the distribution of DR values for LSSSVM-GOA, LSSVM and SVM models in the test period. During this period, the values 1.0155, 1.0734 and 1.1024 for DR_{max} were obtained for LSSVM-GOA, LSSVM and SVM models, respectively. DR_{min} values of 0.8800, 0.8735 and 0.8431 and DR_{ave} values of 0.9878, 0.9818 and 0.9801 were obtained for LSSVM-GOA, LSSVM and SVM models, respectively.

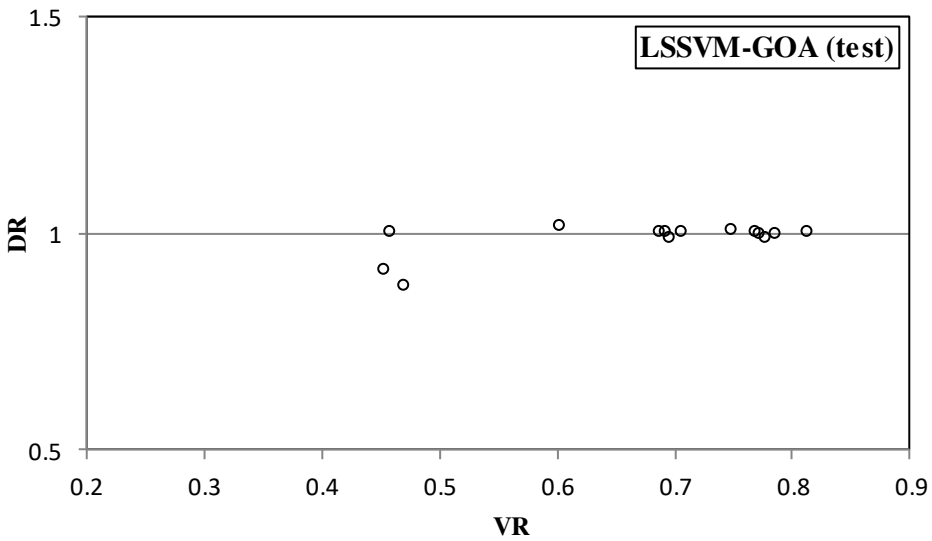

a

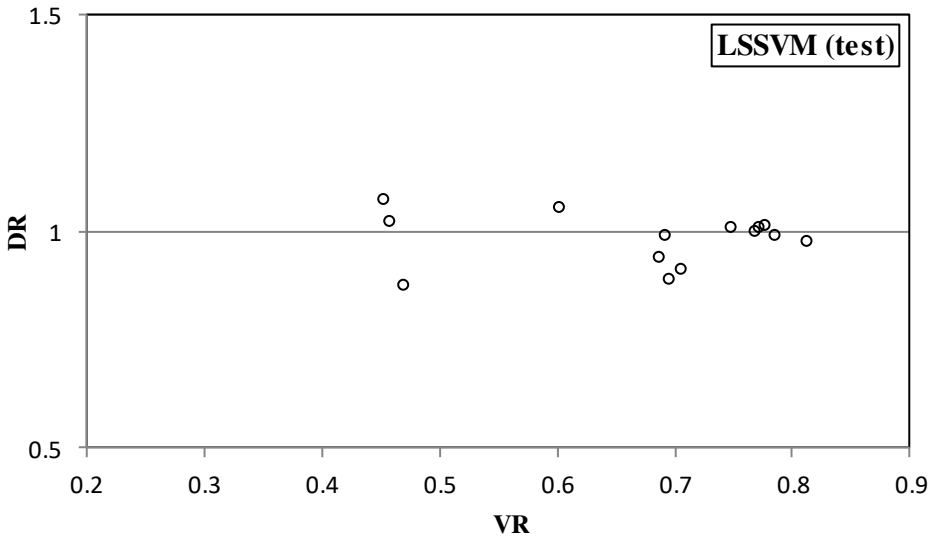

b

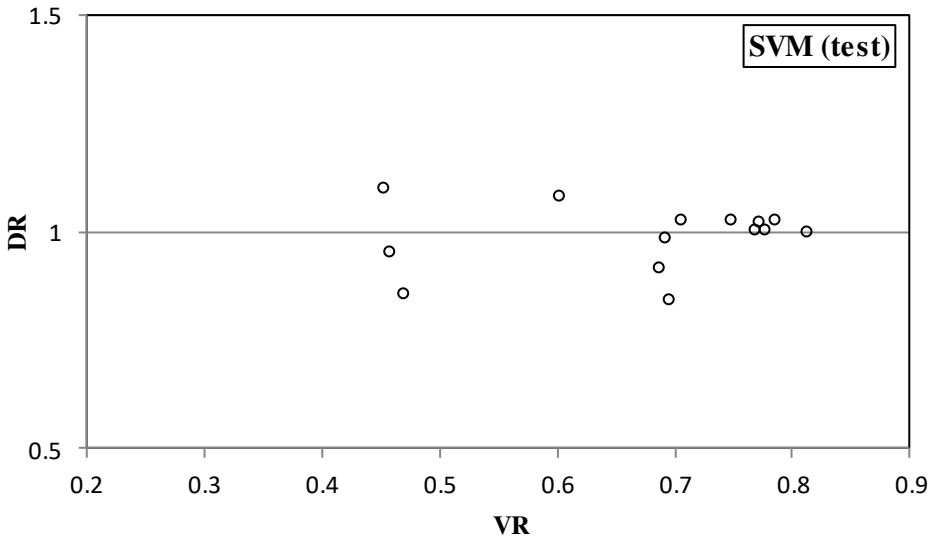

c

Figure 9- DR graphs in the testing phase for models: a) LSSVM-GOA, b) LSSVM, c) SVM

Box diagrams of Volume Reduction (VR) values generated in training and test courses using SVM, LSSVM and LSSVM-GOA models are shown in Figure 10. In each box, a line of two colors (blue and red) represents the middle and the top and bottom edges of the boxes represent

the 75_{th} and 25_{th} percentiles, respectively. As can be seen, in both the training and testing periods, the LSSVM-GOA model can better simulate Volume Reduction (VR) and its distribution is more similar to the observational distribution than other models (75_{th} and 25_{th} percentiles are approximately the same for observational model and LSSVM-GOA model). This indicates the superiority of this method over other models in predicting volume reduction (VR) in both training and testing.

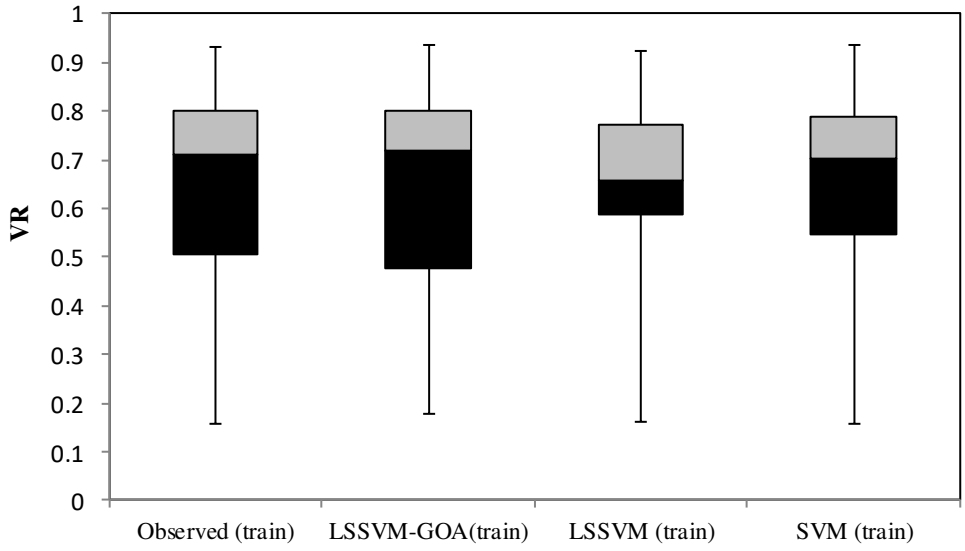

a

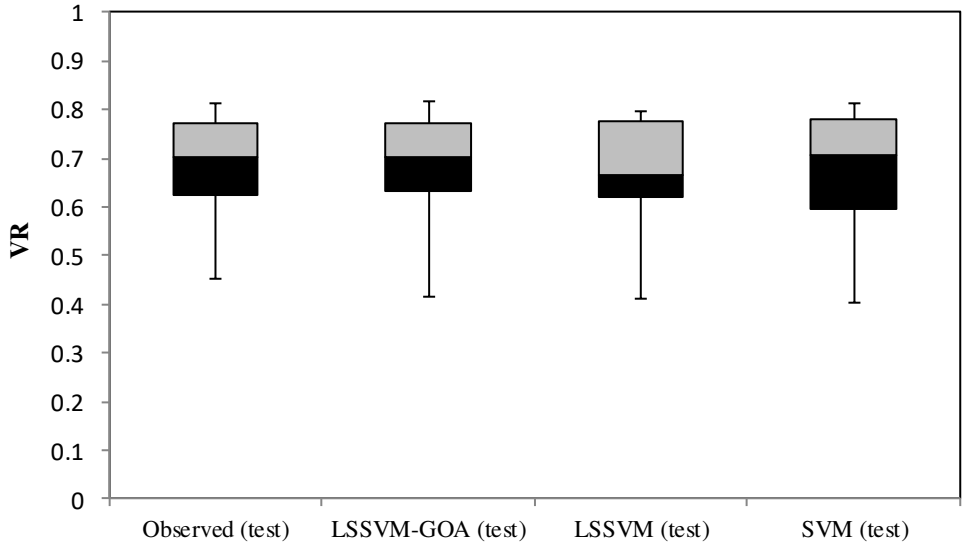

b

Figure 10- Boxplots of observed Volume Reduction compared with predicted Volume Reduction by LSSVM-GOA, LSSVM and SVM models in: a) training phase , b) testing phase

Figure 11 compares the Volume Reduction (VR) in both observational and predictive modes of the LSSVM-GOA, LSSVM and SVM models in the training course. This figure also shows the correlation between the real and estimated data. The results show that in the training course, the data related to the LSSVM-GOA have the highest correlation and the value of 0.9874 has been obtained for this model. After this model, SVM and LSSMV with values of 0.9483 and 0.8977, respectively, are in the next ranks.

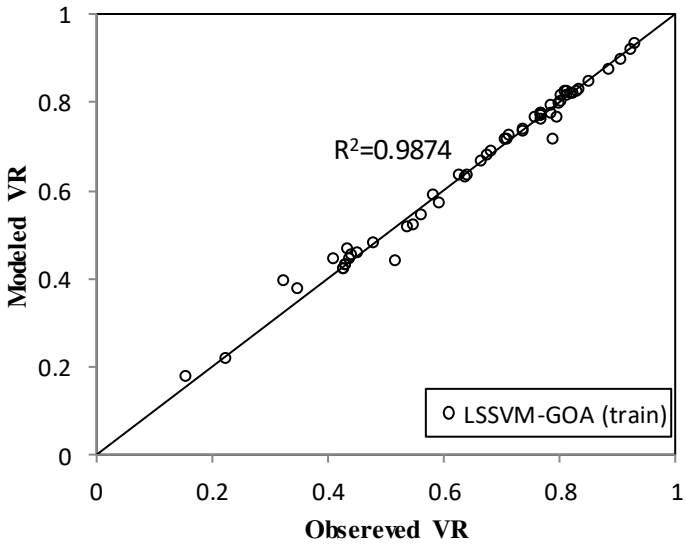

a

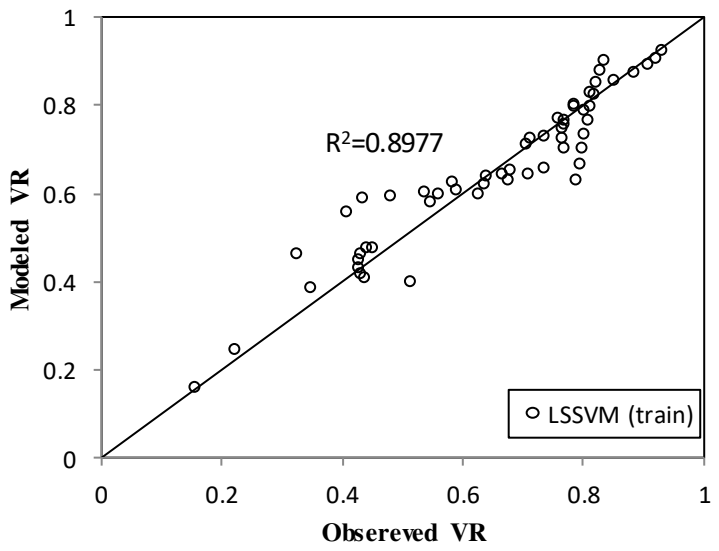

b

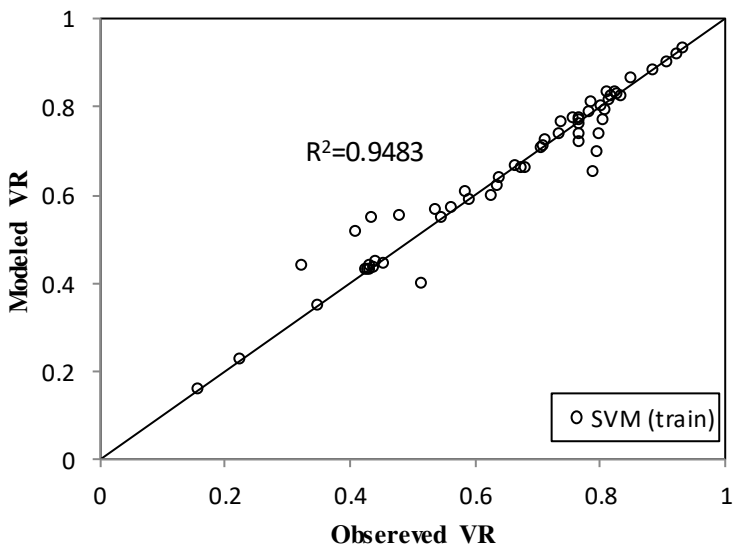

c

Figure 11-The correlation of real and estimated data in the training phase: a) LSSVM-GOA, b) LSSVM, c) SVM

Figure 12 examines the correlation between observational data and the output of LSSVM-GOA, LSSVM and SVM models during the test period. In this period, the LSSVM-GOA model with a correlation coefficient of 0.9896 has shown better performance than the LSSVM with a value of 0.9266 and the SVM model with a value of 0.8990.

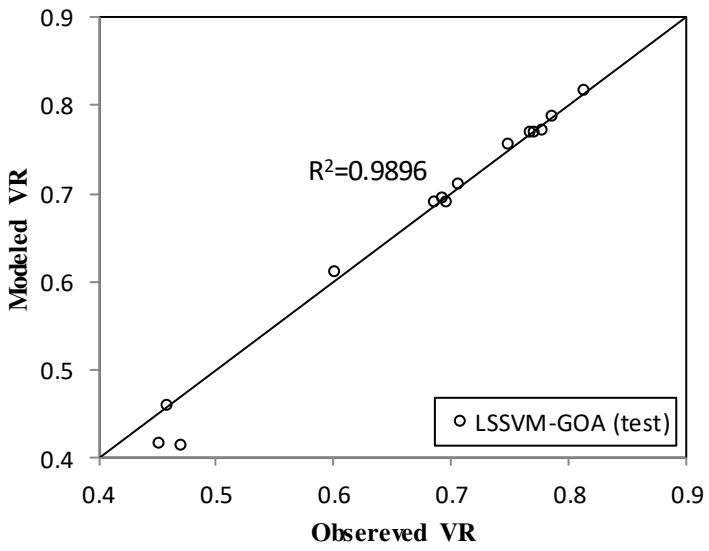
0.9
0.8
0.7
0.6
0.5
0.4
Modeled VR
R2=0.9896
LSSVM-GOA (test)
0.4
0.5
0.6
0.7
0.8
0.9
Obserewed VR

a

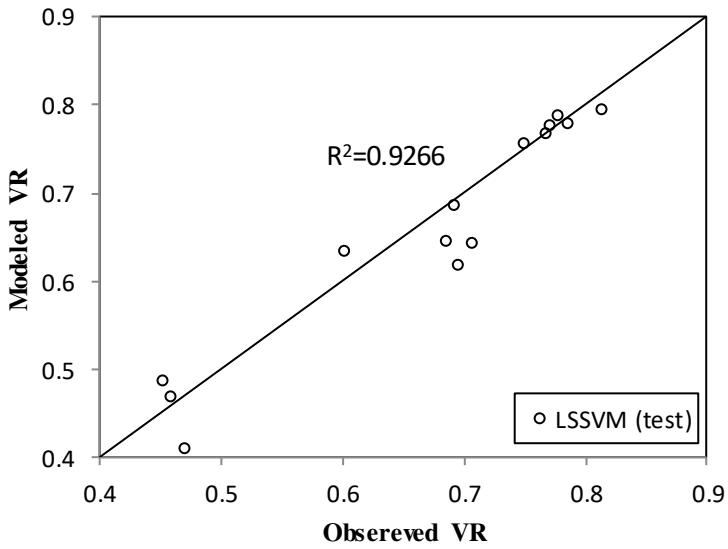
0.9
0.8
0.7
0.6
0.5
0.4
Modeled VR
R2=0.9266
LSSVM (test)
0.4
0.5
0.6
0.7
0.8
0.9
Obserewed VR

b

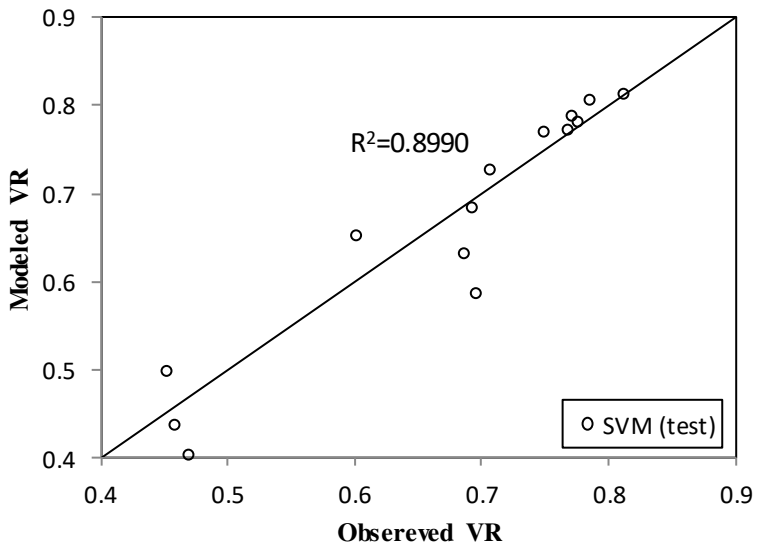

c

Figure 12-The correlation of real and estimated data in the testing phase: a) LSSVM-GOA, b) LSSVM, c) SVM

Figure 13 shows the Taylor diagrams of LSSVM-GOA, LSSVM and SVM (2001) for both train and test. This graph is plotted to compare the results of each algorithm by comparing the value of their standard deviation, correlation coefficient and root mean square error. It should be noted that in Taylor diagram, the longitudinal distance from the origin of the coordinates indicates the standard deviation, the radial lines represent the correlation coefficient and the linear lines show the root mean square error. As the circumference of the circle increases, the value of the mentioned parameter increases. In other words, each point on the Taylor diagram simultaneously represents the three statistical parameters mentioned above. Figure 8 shows that in both training and testing, the LSSVM-GOA has the highest accuracy. Also, LSSVM and SVM models showed the lowest accuracy among the studied models in both train and test stages, respectively.

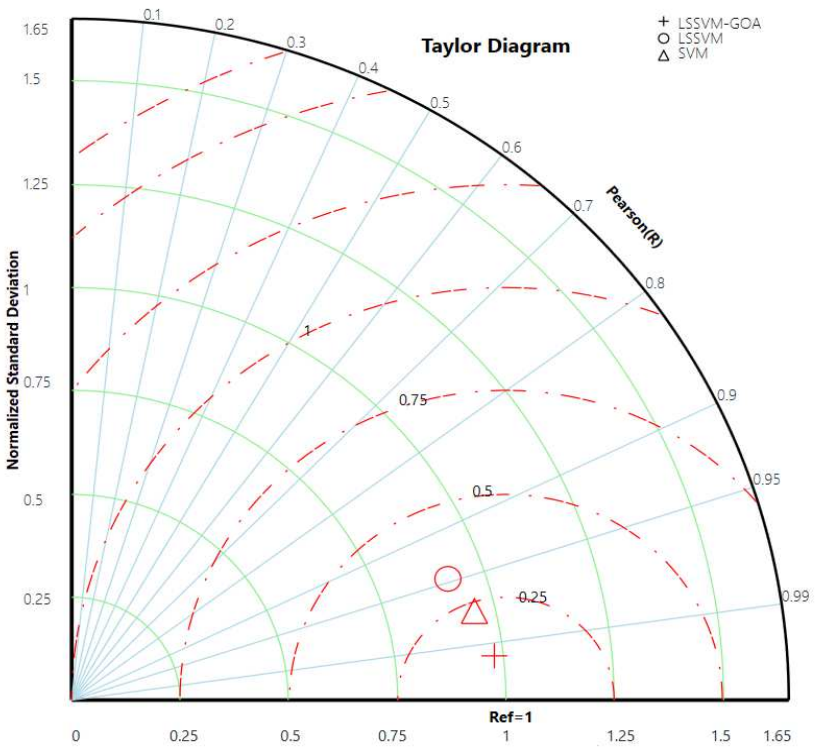

a

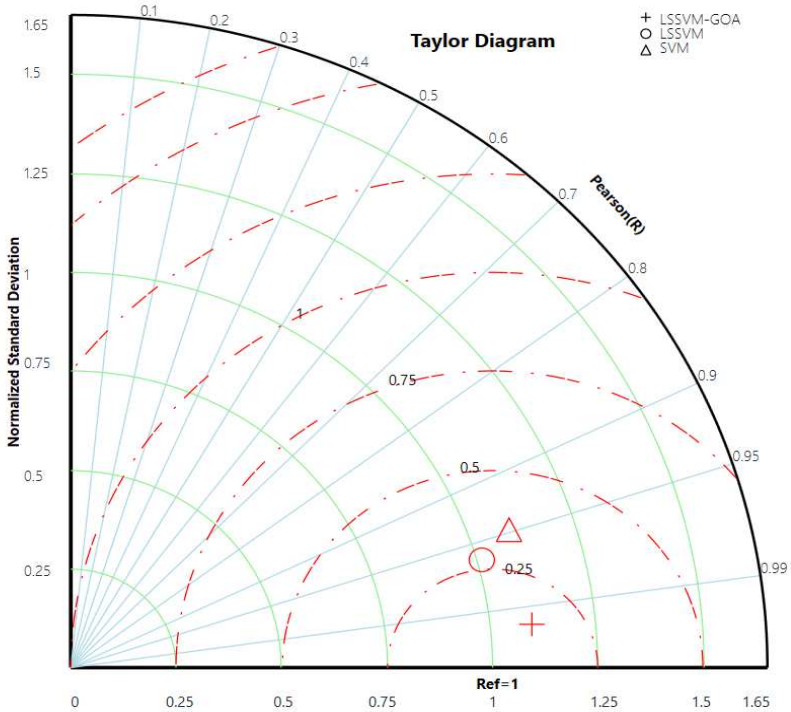

b

Figure 13-Taylor diagrams of predictions in: a) training phase b) testing phase

Conclusion

In this study, after selecting 3 low development methods of rain barrel, permeable pavement, and infiltration trench, 70 different plans under 7 scenarios were introduced. These scenarios include 3 individual scenarios, three paired scenarios, and a triple scenario. The results of SWMM showed that among these 7 scenarios, the PP-RB scenario showed the best results in terms of flood volume reduction and peak discharge reduction. The PP-RB scenario recorded an average of 80% reduction in flood volume and 90% reduction in peak discharge compared to the current system, respectively. Unlike the PP-RB scenario, the IT scenario showed the weakest performance among the 7 scenarios with an average of 60% reduction in peak discharge and 40% reduction in total flood volume

Given the good performance of intelligent methods in this study, it can undoubtedly be concluded that only by estimating the volume of flood required to reduce, it is easy to determine what percentage of low-impact development methods should be selected.

Calculating the reduced volume of floods is one of the goals of designers of urban runoff control systems during heavy rains. Finding the reduced flood rate always requires long calculations and time-consuming modeling, which is not a good method in terms of time and cost due to high calculations. In studies that aim to compare the effectiveness of low-impact development methods in reducing flooding at the basin outlet, we are always dealing with complex modeling for the repetition and application of input data, as well as evaluating the outputs of the SWMM model. The method proposed in this paper using intelligent algorithms SVM, LSSVM, and LSSVM-GOA only by considering the area of the desired LIDs along with the rate of peak discharge reduction has been able to strongly predict the rate of flood reduction in different LID compositions. Hence, it could play a pivotal role in the urban runoff management plans. The results obtained from the simulations performed by these algorithms

indicate that the LSSVM-GOA hybrid algorithm, by showing good performance in statistical criteria, was able to show a powerful simulation in reducing the volume of the flood. The R^2 in the test period for LSSVM-GOA, LSSVM and SVM algorithms is 0.9896, 0.9266 and 0.8990, respectively. The numbers obtained indicate the power of all three algorithms in predicting flood reduction volume, but the predictive power of the LSSVM-GOA algorithm is quite obvious compared to the other two algorithms. Also, in test period, LSSVM - GOA model showed higher predictive power that with values of 0.0101 and 0.0185 compared to LSSVM model with values of 0.0268 and 0.0361 and SVM model with values of 0.0318 and 0.0434 for MAE and RMSE indices, respectively.

Also, the high correlation of all three algorithms indicates the high power of all three in predicting the reduced flood volume, while in the training period, the data related to the LSSVM-GOA model have the highest correlation and density among the studied models (correlation coefficient of 0.9874). These results show that the LSSVM-GOA hybrid algorithm has a good ability to predict the rate of flood reduction. In other words, the proposed method in this research has much less limitations in terms of time and cost of modeling compared to conventional modeling methods such as using the SWMM method, and the results obtained are also suitable for using designs related to control systems of urban flooding.

In the following, it is suggested to use smart methods to study the best places to implement low-impact development methods in order to control floods.

Ethical Approval

Not applicable

Consent to Participate

Authors consent to their participation in the entire review process.

Consent to Publish

Authors allow publication if the research is accepted.

Authors Contributions

Conceptualization: Yashar Dadrasajirlou, Hojat karami, Alireza rezaei

Writing-original draft preparation: Yashar Dadrasajirlou, Alireza rezaei

Review and editing: Yashar Dadrasajirlou, Hojat karami

Methodology: Yashar Dadrasajirlou, Hojat karami, Alireza rezaei

Data curation: Yashar Dadrasajirlou, Hojat karami, Alireza rezaei

Formal analysis: Yashar Dadrasajirlou, Hojat karami

Funding:

Not Funded

Conflicts of Interests

The authors declare no conflicts of interest.

Availability of data and materials

The data could be available by an official email to hkarami@semnan.ac.ir

Reference

Aghelpour, P., kisi, O., Varahvian, V. 2021. Multivariate Drought Forecasting in Short- and Long-Term Horizons Using MSPI and Data-Driven Approaches. Journal of hydrologic engineering. 26(4) April 2021. https://doi.org/10.1061/(ASCE)HE.1943-5584.0002059

Anaraki, M.V., Farzin, S, Mousavi, SF., Karami, H. 2021. Uncertainty Analysis of Climate Change Impacts on Flood Frequency by Using Hybrid Machine Learning Methods. Water Resources Management: An International Journal, Published for the European Water Resources Association (EWRA), Springer; European Water Resources Association (EWRA). 35(1): 199-223. DOI: 10.1007/s11269-020-02719-w

Azad, A., Farzin, S., Sanikhani, H., Karami, H., kisi, O., Singh, VP. 2021. Approaches for Optimizing the Performance of Adaptive Neuro-Fuzzy Inference System and Least-Squares Support Vector Machine in Precipitation Modeling. Journal of hydrologic engineering. 26(4). April 2021. https://doi.org/10.1061/(ASCE)HE.1943-5584.0002069

Anandhi, A., Srinivas, V.V., Nanjundiah, R.S., Kumar, D.N., (2008). Downscaling precipitation to river basin in India for IPCC SRES scenarios using support vector machine, *International Journal of Climatology*, 28(3), 401-20.

Ahiablame, L.M., Engel, B.A., Chaubey, I., 2012. Effectiveness of low impact development practices: literature review and suggestions for future research. Water Air Soil Pollut. 223 (7), 4253-4273. https://doi.org/10.1007/s11270-012-1189-2

Behza, M., Asghari, K., Eazi, M., Palhang, M. 2009. Generalization performance of support vector machines and neural networks in runoff modeling. Expert Systems with Applications. 36(4): 7624-7629. https://doi.org/10.1016/j.eswa.2008.09.053

Bond, N., et al., 2014. Ecological risks and opportunities from engineered artificial flooding as a means of achieving environmental flow objectives. Front. Ecol. Environ. 12 (7), 386–394. https://doi.org/10.1890/130259.

Babaei, S. Ghazavi, R. Erfanian, M., 2018, Urban flood simulation and prioritization of critical urban sub-catchment using SWMM model and PROMETHEE II approach, Physics and chemistry of the earth, 105(2018):3-11. https://doi.org/10.1016/j.pce.2018.02.002

Bisht, D.S., Chatterjee, C., Kalakoti, S., et al., 2016. Modeling urban floods and drainage using SWMM and MIKE URBAN: a case study. Nat. Hazards, 84:749–776 (2016). https://doi.org/10.1007/s11069-016-2455-1

Chen, ST., Yu, PS., Tang, YH. 2010. Statistical downscaling of daily precipitation using support vector machines and multivariate analysis. Journal of Hydrology. 385(1-4): 13-22. https://doi.org/10.1016/j.jhydrol.2010.01.021

Choubin, B.; Moradi, E.; Golshan, M.; Adamowski, J.; Sajedi-Hosseini, F.; Mosavi, A. An Ensemble prediction of flood susceptibility using multivariate discriminant analysis, classification and regression trees, and support vector machines. Elsevier Sci. Total Environ. 2018, 651, 2087–2096. https://doi.org/10.1016/j.scitotenv.2018.10.064

Dietz, M.E., Clausen, J.C., 2008. Stormwater runoff and export changes with development in a traditional and low impact subdivision. J. Environ. Manag. 87(4): 560–566. https://doi.org/10.1016/j.jenvman.2007.03.026

Eckart, J., Sieker, H., Vairavamoorthy, K., Alsharif, K., 2012. Flexible design of urban drainage systems: demand led research for Hamburg-Wilhelmsburg. Rev. Environ.Sci. Biotechnol. 11 (1), 5-10. https://doi.org/10.1007/s11157-011-9256-5.

Elliott, A.H., Trowsdale, S.A., 2007. A review of models for low impact urban storm water drainage. Environ. Model. Softw. 22 (3), 394-405. https://doi.org/10.1016/j.envsoft.2005.12.005

Faye M, Vb Traore, Bob M, Al Et (2016) Hydrologic modeling in diass river basin using rainfall. Int J Recent Sci Res 6:7290-7295.

Flood, J., 1997. Urban and housing indicators. Urban Stud. 34, 1635–1665. https://doi.org/10.1080%2F0042098975385

Fiori, A., Volpi, E., 2020. On the effectiveness of LID infrastructures for the attenuation of urban flooding at the catchment scale. Water Resour. Res. 56 (5) e2020WR027121. https://doi.org/10.1029/2020WR027121

Fu, X., Hopton, M.E., Wang, X., Goddard, H., Liu, H., 2019. A runoff trading system to meet watershed-level stormwater reduction goals with parcel-level green infrastructure installation. Sci. Total Environ. 689, 1149e1159. https://doi.org/10.1016/j.scitotenv.2019.06.439

Freer, J., et al., 2013. Flood risk and uncertainty. Cambridge University Press, UK. Gass, S.I., 1983. Decision-aiding models: validation, assessment, and related issues for policy analysis. Oper. Res. 31 (4), 603–631. https://doi.org/10.1017/CBO9781139047562.008

Goel, A., Pal, M. 2009. Application of support vector machines in scour prediction on grade-control structures. Engineering Applications of Artificial Intelligence. 22(2): 216-223. https://doi.org/10.1016/j.engappai.2008.05.008

Gill, MK., Asefa, T., Kemblowski, MW., McKee, M. 2007. SOIL MOISTURE PREDICTION USING SUPPORT VECTOR MACHINES. Journal of the American Water Resources Association. 42(4): 1033-1046. https://doi.org/10.1111/j.1752-1688.2006.tb04512.x

Geng, R., Sharpley, A.N., 2019. A novel spatial optimization model for achieve the trade-offs placement of best management practices for agricultural non-point source pollution control at multi-spatial scales. Clean. Prod. 234, 1023-1032. https://doi.org/10.1016/j.jclepro.2019.06.277.

Ghazavi, R., Vali, A., Eslamian, S., 2012. Impact of flood spreading on groundwater level variation and groundwater quality in an arid environment. Water Resour. Manag. 26, 1651–1663(2012). https://doi.org/10.1007/s11269-012-9977-4

Hoang, L., Fenner, R.A., 2016. System interactions of stormwater management using sustainable urban drainage systems and green infrastructure. Urban Water J. 13 (7), 739-758. https://doi.org/10.1080/1573062X.2015.1036083.

Huang, C.-L., Hsu, N.-S., Liu, H.-J., Huang, Y.-H., 2018. Optimization of low impact development layout design for megacity flood mitigation. J. Hydrol. 564,542e558. https://doi.org/10.1016/j.jhydrol.2018.07.044.

HUD (U.S. Department of Housing and Urban Development), 2003. The Practice of Low Impact Development. Office of Policy Development and Research, Washington, D.C. Report prepared by NAHB Research Center, Inc. Contract No. H21314CA. https://www.huduser.gov/publications/pdf/practlowimpctdevel.pdf

Henonin, J., Hongtao, M., Zheng-Yu, Y., Hartnack, J., Havnø, K., Gourbesville, P., Mark, O., 2015. Citywide multi-grid urban flood modelling: the July 2012 flood in Beijing. Urban Water J. 12 (1), 52e66. https://doi.org/10.1080/1573062X.2013.851710

Jacobson, C.R., 2011. Identification and quantification of the hydrological impacts of imperviousness in urban catchments: a review. J. Environ. Manag. 92(6): 1438–1448. https://doi.org/10.1016/j.jenvman.2011.01.018

Jia, H.; Yao, H.; Tang, Y.; Yu, S.L.; Zhen, J.X.; Lu, Y. 2013,Development of a multi-criteria index ranking system for urban runoff best management practices (BMPs) selection. Environ. Monit. Assess., 185(2013): 7915–7933. https://doi.org/10.1007/s10661-013-3144-0

Karami H, DadrasAjirlou Y, Jun C, Bateni SM, Band SS, Mosavi A, Moslehpour M and Chau K-W (2022) A Novel Approach for Estimation of Sediment Load in Dam Reservoir With Hybrid Intelligent Algorithms. *Front. Environ. Sci.* 10:821079. doi: 10.3389/fenvs.2022.821079

Kayhanian, M., Fruchtman, B.D., Gulliver, J.S., Montanaro, C., Ranieri, E., Wuertz, S., 2012. Review of highway runoff characteristics: comparative analysis and universal implications. Water Res. 46 (20), 6609-6624. https://doi.org/10.1016/j.watres.2012.07.026

Lawson, E., Thorne, C., Ahilan, S., Allen, D., Arthur, S., Everett, G., Fenner, R., Glenis, V., Guan, D., Hoang, L., 2014. Delivering and Evaluating the Multiple Flood Risk Benefits in Blue-Green Cities: an Interdisciplinary Approach. WIT Press. https://scholar.google.com/scholar_lookup?title=Delivering%20and%20Evaluating%20the%20Multiple%20Flood%20Risk%20Benefits%20in%20Blue-

Green%20Cities%3A%20an%20Interdisciplinary%20Approach&author=E.%20Lawson&publication_year=2014

Li, L., Uyttenhove, P., Vaneetvelde, V., 2020. Planning green infrastructure to mitigate urban surface water flooding risk e a methodology to identify priority areas applied in the city of Ghent. Landsc. Urban Plann. 194, 103703. https://doi.org/10.1016/j.landurbplan.2019.103703

Liu, Y., Ji, Y., Liu, D., Fu, Q., Li, T., Hou, R., Li, Q., Cui, S., Li, M. 2021. A new method for runoff prediction error correction based on LS-SVM and a 4D copula joint distribution. Journal of hydrology. 598 July 2021. https://doi.org/10.1016/j.jhydrol.2021.126223

Maharjan B, Pachel K,Loigu E (2017) Modelling stormwater runoff, quality, and pollutant loads in a large urban catchment. Proc Est Acad Sci 66:225. https://doi.org/10.3176/proc.2017.3.02

Martin-Mikle, C.J., Beurs, K.M., Julian, J.P., Mayer, P.M., 2015. Identifying priority sites for low impact development (LID) in a mixed-use watershed. Landsc. Urban Plan. 140, 29-41. https://doi.org/10.1016/j.landurbplan.2015.04.002.

Misra, D., Oommen, T., Agarwal, A., Mishra, S. 2009. Application and analysis of support vector machine based simulation for runoff and sediment yield. Biosystems Engineering 103(4):527-535. http://dx.doi.org/10.1016/j.biosystemseng.2009.04.017

Mark, O., Weesakul, S., Apirumanekul, C., Aroonnet, S.B., Djordjevic, S., 2004. Potential and limitations of 1D modelling of urban flooding. J. Hydrol. 299 (3e4),284e299. https://doi.org/10.1016/j.jhydrol.2004.08.014

Miguez, M.G., Battemarco, B.P., De Sousa, M.M., Rezende, O.M., Verol, A.P., Gusmaroli, G., 2017. Urban flood simulation using MODCELAn alternative quasi2D conceptual model. Water 9 (6). https://doi.org/10.3390/w9060445

Olang, L.O., Furst, J., 2011. Effects of land cover change on flood peak discharges and runoff volumes: model estimates for the Nyando River Basin, Kenya. Hydrol. Process. 25 (1), 80e89. https://doi.org/10.1002/hyp.7821

Palla, A., Gnecco, I., 2015. Hydrologic modeling of Low Impact Development systems at the urban catchment scale. J. Hydrol. 528, 361–368. https://doi.org/10.1016/j.jhydrol.2015.06.050

Park, D., Song, Y.I., Roesner, L.A., 2013. Effect of the seasonal rainfall distribution on storm-water quality capture volume estimation. J. Water Resour. Plan. Manag. 139 (1), 45-52. https://doi.org/10.1061/(ASCE)WR.1943-5452.0000204

Prez-Pedini, C., Limbrunner, J., Wogel, R., 2005. Optimal location of infiltration based best management practices for storm water management. J. Water Resour. Plan. Manag. 131(6): 441-448. https://doi.org/10.1061/(ASCE)0733-9496(2005)131:6(441)

Pham, QB., Yang, TC., Kou, CM., Tseng, HW., Yu, PS. 2021. Coupling Singular Spectrum Analysis with Least Square Support Vector Machine to Improve Accuracy of SPI Drought Forecasting. Water Resources Management: An International Journal, Published for the European Water Resources Association (EWRA), Springer; European Water Resources Association (EWRA). 35(3): 847-868. DOI: 10.1007/s11269-020-02746-7

Panahi, M., Dodangh, E., Rezaie, F., Khosravi, K., Le, HV. Lee, MJ., LEE, S., Pham, T. 2021. Flood spatial prediction modeling using a hybrid of meta-optimization and

support vector regression modeling. CATENA. 199,105114. https://doi.org/10.1016/j.catena.2020.105114

Pappalardo, V., La Rosa, D., Campisano, A., La Greca, P., 2017. The potential of green infrastructure application in urban runoff control for land use planning: a preliminary evaluation from a southern Italy case study. Ecosystem Services 26, 345e354. https://doi.org/10.1016/j.ecoser.2017.04.015

Randhir, T.O., Raposa, S., 2014. Urbanization and watershed sustainability: collaborative simulation modeling of future development states. J. Hydrol. 519(part B):1526-1536. https://doi.org/10.1016/j.jhydrol.2014.08.051

Razavi, S., Gober, P., Maier, H.R., Brouwer, R., Wheater, H., 2020. Anthropocene flooding: Challenges for science and society. Hydrol. Process. 34 (8), 1996–2000. https://doi.org/10.1002/hyp.13723.

Rene, J.-R., Djordjevic, S., Butler, D., Madsen, H., Mark, O., 2014. Assessing the potential for real-time urban flood forecasting based on a worldwide survey on data availability. Urban Water J. 11 (7), 573e583. https://doi.org/10.1080/1573062X.2013.795237

Song, C., Yao, L., Hua, C., Ni, Q. 2021. A water quality prediction model based on variational mode decomposition and the least squares support vector machine optimized by the sparrow search algorithm (VMD-SSA-LSSVM) of the Yangtze River, China. Environ Monit Assess. 2021 May 27;193(6):363. doi: 10.1007/s10661-021-09127-6.

Suykens, J.A. (2001). Nonlinear modelling and support vector machines, In Instrumentation and Measurement Technology Conference, 2001, IMTC 2001, 1 Proceedings of the 18th IEEE. 287-294.

Saremi, S., Mirjalili, S and Lewis, A. 2017. Grasshopper optimisation algorithm: theory and application. Adv Eng Softw. 105: 30–47

Schoonover, J.E., Lockaby, B.G., Helms, B.S., 2006. Impacts of land cover on stream hydrology in the west Georgia piedmont, USA. J. Environ. Qual. 35(6): 2123–2131. https://doi.org/10.2134/jeq2006.0113

Shahed Behrouz M, Zhu Z, Matott LS, Rabideau AJ (2020) A new tool for automatic calibration of the Storm water Management Model (SWMM). J Hydrol 581: 124436. https://doi.org/10.1016/j.jhydrol.2019.124436

Shen, Z., Hou, X., Li, W., Aini, G., 2014. Relating landscape characteristics to nonpoint source pollution in a typical urbanized watershed in the municipality of Beijing. Landsc. Urban Plan. 123 (96), 107. https://doi.org/10.1016/j.landurbplan.2013.12.007.

Tao, H., Al-Bedyry, NK., Khedher, KM., Shahid, S., Yaseen, ZM. 2021. River water level prediction in coastal catchment using hybridized relevance vector machine model with improved grasshopper optimization. Journal of Hydrology. 598, 126477. https://doi.org/10.1016/j.jhydrol.2021.12647

Teng, J., et al., 2017. Flood inundation modelling: A review of methods, recent advances and uncertainty analysis. Environ. Modell. Software 90, 201–216. https://doi.org/10.1016/j.envsoft.2017.01.006

Tezel, G., Buyukyildiz, M. 2015. Monthly evaporation forecasting using artificial neural networks and support vector machines. Theoretical and Applied Climatology. 124, pages69–80 (2016). https://doi.org/10.1007/s00704-015-1392-3

Teymouri, E. Mousavi, S-F. Karami, H. Farzin, S. Kheirabad, H., 2020, Reducing Urban Runoff Pollution Using Porous Concrete Containing Mineral Adsorbents, J. Environ.

Treat. Tech, 8(1):429-436. http://www.jett.dormaj.com/docs/Volume8/Issue%201/Reducing%20Urban%20Runoff%20Pollution%20Using%20Porous%20Concrete%20Containing%20Mineral%20Adsorbents.pdf

UN, U., 2012. World Urbanization Prospects: the 2011 Revision: United Nations. Department of Economic and Social Affairs. Population Division. https://www.un.org/en/development/desa/population/publications/pdf/urbanization/WUP2011_Report.pdf

Vapnik, V.N. 1995.The Nature of Statistical Learning Theory. Springer, New York.

Wang, Y., Choi, W., Deal, B.M., 2005. Long-term impacts of land-use change on non-point source pollutant loads for the St. Louis metropolitan area, USA. Environ. Manag. 35, 194–205. https://doi.org/10.1007/s00267-003-0315-8

Wolch, J.R., Byrne, J., Newell, J.P., 2014. Urban green space, public health, and environmental justice: the challenge of making cities 'just green enough'. Landsc. Urban Plann. 125, 234e244. https://doi.org/10.1016/j.landurbplan.2014.01.017

Yoon, H., Jun, S-C., Hyun, Y., Bae, G-O., Lee, K-K. 2011. A comparative study of artificial neural networks and support vector machines for predicting groundwater levels in a coastal aquifer. Journal of Hydrology. 936(1-2): 128-138. https://doi.org/10.1016/j.jhydrol.2010.11.002

Zhang, B., Xie, G.-d., Li, N., Wang, S., 2015. Effect of urban green space changes on the role of rainwater runoff reduction in Beijing, China. Landsc. Urban Plann. 140, 8e16, 0. https://doi.org/10.1016/j.landurbplan.2015.03.014

Zhang, W., Villarini, G., Vecchi, G.A., Smith, J.A., 2018. Urbanization exacerbated the rainfall and flooding caused by hurricane Harvey in Houston. Nature 563(7731), 384e388. https://doi.org/10.1038/s41586-018-0676-z